


RESEARCH ARTICLE

Central encoding of the strength of intranasal chemosensory trigeminal stimuli in a human experimental pain setting

Jörn Lötsch^{1,2}  | Bruno G. Oertel¹ | Lisa Felden¹ | Ulrike Nöth³ | Ralf Deichmann³ | Thomas Hummel⁴ | Carmen Walter^{1,2}

¹Institute of Clinical Pharmacology, Goethe – University, Frankfurt am Main, Germany

²Fraunhofer Institute for Molecular Biology and Applied Ecology IME, Branch for Translational Medicine and Pharmacology TMP, Frankfurt am Main, Germany

³Brain Imaging Center, Goethe – University, Frankfurt am Main, Germany

⁴Smell & Taste Clinic, Department of Otorhinolaryngology, TU Dresden, Dresden, Germany

Correspondence

Jörn Lötsch, Goethe – University, Theodor – Stern – Kai 7, 60590 Frankfurt am Main, Germany. Email: j.loetsch@em.uni-frankfurt.de

Funding information

Deutsche Forschungsgemeinschaft, Grant/Award Number: DFG Lo 612/11-1

Abstract

An important measure in pain research is the intensity of nociceptive stimuli and their cortical representation. However, there is evidence of different cerebral representations of nociceptive stimuli, including the fact that cortical areas recruited during processing of intranasal nociceptive chemical stimuli included those outside the traditional trigeminal areas. Therefore, the aim of this study was to investigate the major cerebral representations of stimulus intensity associated with intranasal chemical trigeminal stimulation. Trigeminal stimulation was achieved with carbon dioxide presented to the nasal mucosa. Using a single-blinded, randomized crossover design, 24 subjects received nociceptive stimuli with two different stimulation paradigms, depending on the just noticeable differences in the stimulus strengths applied. Stimulus-related brain activations were recorded using functional magnetic resonance imaging with event-related design. Brain activations increased significantly with increasing stimulus intensity, with the largest cluster at the right Rolandic operculum and a global maximum in a smaller cluster at the left lower frontal orbital lobe. Region of interest analyses additionally supported an activation pattern correlated with the stimulus intensity at the piriform cortex as an area of special interest with the trigeminal input. The results support the piriform cortex, in addition to the secondary somatosensory cortex, as a major area of interest for stimulus strength-related brain activation in pain models using trigeminal stimuli. This makes both areas a primary objective to be observed in human experimental pain settings where trigeminal input is used to study effects of analgesics.

KEYWORDS

data science, experimental human pain models, functional imaging, trigeminal pain

1 | INTRODUCTION

Experimental human pain models are established tools for the study of human nociception and analgesic drug effects (Bingel & Tracey, 2008;

Handwerker & Kobal, 1993). If carefully chosen, they may even predict clinical analgesia satisfactorily (Lötsch, Oertel, & Ultsch, 2014; Oertel & Lotsch, 2013). Pain models involve two main components comprising (a) the application of nociceptive stimuli and (b) the recording of

This is an open access article under the terms of the Creative Commons Attribution-NonCommercial-NoDerivs License, which permits use and distribution in any medium, provided the original work is properly cited, the use is non-commercial and no modifications or adaptations are made.

© 2020 The Authors. *Human Brain Mapping* published by Wiley Periodicals LLC.

responses to the stimuli. For the implementation of both components, numerous techniques has been proposed (Handwerker & Kopal, 1993; Lötsch et al., 2014), raising already 70 years ago the need for defining basic requirements (Beecher, 1957).

One of the most important features is the correlation between the physical strength of the stimulus and the perceived intensity of the evoked pain. The interaction between the two is one of the most important objectives in the experimental evaluation of the effect of analgesic drugs. The latter are quantified either as an increase in the physical strength of the stimulus required to produce the same intensity of pain or as a decrease in the intensity of pain caused by the same stimulus before the drug is administered. The subjective perception of different pain intensities is an essential criterion for a therapeutic effect on pain. Improvements are usually quantified by evaluating the reduced pain intensity.

Considering the importance of perceiving stimuli of different strength as differently painful, two stimulation paradigms were compared in the present study, comprising stimuli of different intensities, with intensity differences either above or below the just noticeable difference (JND) (Fechner, 1860). This was addressed by employing painful chemical stimuli, that is, intranasal trigeminal excitation by gaseous carbon dioxide (Kopal, 1981, 1985), which has been shown previously in a comparative computational analysis (Lötsch et al., 2014) of human experimental pain models to yield best results with regard to correct prediction of clinical analgesic drug effects. A special feature of this pain model is the use of intranasal trigeminal pain, which has been shown to have unique features of brain activation related to the close interactions of the intranasal trigeminal chemosensory system with the olfactory system (Hummel & Livermore, 2002). Cortical areas recruited during processing of intranasal CO₂ stimuli included those outside the traditional trigeminal areas and overlapped significantly between brain areas processing trigeminal and olfactory information (Albrecht et al., 2010).

The objectives of this study were therefore to investigate the most important cerebral representations of the stimulus intensity of intranasal chemosensory trigeminal stimuli, with special emphasis on the particular findings about brain activation associated with the specific stimuli in the context of the present experimental pain model.

2 | METHODS

2.1 | Study design and setting

A single-blinded single-occasion randomized crossover design was employed to assess the two different stimulation paradigms. Specifically, during the “distinct stimuli” condition, a total of 80 nociceptive stimuli of four different strengths above the pain threshold were applied at a randomized order. The differences in strength exceeded the JND to render the stimuli clearly distinguishable. During the “non-distinct stimuli” condition, a total of 80 stimuli of 19 different strengths were applied at a randomized order. All stimuli were above the pain threshold; however, the increment in stimulus strength was

below the JND, so subsequent stimuli were not clearly distinguishable. The two paradigms were applied at random succession in each subject at the same day, with a 20-min interval between the assessments.

2.2 | Participants

Twenty-four healthy subjects were enrolled. The subjects' good health was assessed by a short physical examination including vital signs and querying medical history. Before the experiments, medications were prohibited for 1 week except oral contraceptives, and alcohol intake was not allowed for 24 hr.

The study followed the Declaration of Helsinki and was approved by the Ethics Committee of the Goethe University, Frankfurt am Main, Germany. Informed written consent from each participating subject had been obtained.

2.3 | Objectives

The study aimed to identify the most important cerebral representations of the stimulus intensity of intranasal chemosensory trigeminal stimuli. Several lines of evidence pointed to certain cortical representations of intranasal chemosensory trigeminal stimuli, possibly based on close interactions with the olfactory system. The analysis focused on establishing a robust association of stimulus perception with stimulus intensity and used this association to freely evaluate associated brain activations, focusing on specific regions of interest such as the secondary somatosensory area or the piriform cortex as representatives of general pain-related cortical activity and specific trigeminal chemosensory activities.

2.3.1 | Variables and measurements experimental induction of pain

Experimentally induced pain consisted of short stinging sensations evoked by stimulating trigeminal nerve endings at the nasal mucosa via local administration of short pulses of gaseous carbon dioxide (CO₂) (Kopal, 1981, 1985). This specifically activated nociceptors (Anton, Euchner, & Handwerker, 1992) of trigeminal sensory neurons projecting into the nasal mucosa (Steen, Reeh, Anton, & Handwerker, 1992). The stimuli were administered into the subject's right nostril using an olfactometer (Kopal, 1981) (OM/2, Burghart Instruments, Wedel, Germany), which allowed for a precise control of the following stimulus parameters: CO₂ concentration, constant duration of 500 ms, steepness of onset (raise time < 50 ms) and air-flow (8 L/min) in which the CO₂ stimuli were embedded.

During each study condition, a total of 80 CO₂ stimuli of different intensities ranging from 50 to 77% vol/vol was applied intranasally. These CO₂ concentrations were chosen based on previous observations that they evoke sensations well above the pain threshold

(Hummel, Mohammadian, Marchl, Kobal, & Lötsch, 2003; Oertel et al., 2012). The interstimulus interval was randomly chosen between 13.5 and 28.2 s, which sufficed to minimize habituation effects (Hummel & Kobal, 1999). During the “distinct stimuli” condition, the 80 stimuli comprised four different strengths (50, 59, 68, and 77% vol/vol CO₂, $n = 20$ each). The CO₂ concentration interval of 9% vol/vol exceeds previously identified JND levels of the CO₂ stimuli. Specifically, a study on 12 subjects, using stimulus concentrations of 50, 60, and 70% vol/vol CO₂ and stimulus durations of 200, 400, 800, and 1,600 ms, had shown that JNDs ranged from $1.9 \pm 0.9\%$ vol/vol CO₂ for stimuli of 50% vol/vol with a duration of 200 ms to $5.5 \pm 2\%$ vol/vol for CO₂ stimuli of 70% vol/vol with a duration of 1,600 ms (Hummel et al., 2003). In an independent experiment, using electrophysiological recordings from the nasal mucosa, a JND of 3% vol/vol was reported (Thürauf, Ditterich, & Kobal, 1994). By contrast, during the “non-distinct stimuli” condition, the 80 stimuli comprised 19 different strengths between 50 and 77% vol/vol at concentration intervals of 1.5% vol/vol, which was less than JND levels reported in the cited studies. In addition, during each condition, 20 blank stimuli (CO₂ = 0% vol/vol) were randomly interspersed.

2.3.2 | Assessment of stimulus associated bioresponses

Query of stimulus-related pain perceptions

Subjects rated the evoked pain intensity on a 100-mm visual analog scale (VAS) displayed randomly within 3.4–6.6 s after stimulus presentation and ranging from 0 mm (“no pain”) to 100 mm (“pain experienced at a maximum”). Secondary assessments addressed the stimulus pleasantness, rated on a VAS ranging from 0 mm (“very unpleasant”) to 100 mm (“very pleasant”) with neutral hedonics corresponding to a rating of 50 mm. Pain intensity and stimulus pleasantness were queried alternately. Hence, 40 ratings, each of pain or stimulus pleasantness, were queried. This design was chosen to limit the duration of the fMRI session while providing sufficient MRI acquisitions per stimulus strength.

Recording of stimulus-related brain activations

Employing an event-related design (Friston et al., 1998), the blood-oxygenation level dependent (BOLD [Ogawa, Lee, Kay, & Tank, 1990]) response to the pain stimuli was recorded on a 3-T-MR head scanner (Siemens Magnetom Allegra, Siemens Medical Solutions, Erlangen, Germany) equipped with a combined single channel transmit and 4-channel receive head coil. The subject's head was immobilized with foam pads. In each session, 920 volumes (32 slices, 3 mm thick, 1 mm inter-slice gap, descending order) were recorded using a T2*-weighted gradient echo (GE) echo planar imaging (EPI) sequence (TR = 2048 ms, TE = 30 ms, flip angle = 90°, echo spacing = 420 μ s, matrix size = 64×64 , field of view [FoV] = 192×192 mm², and in-plane resolution = 3×3 mm²). Following EPI acquisition, distortions of the static magnetic field were assessed (Andersson, Hutton, Ashburner, Turner, & Friston, 2001; Hutton et al., 2002) by acquiring

GE images with identical geometric parameters and two different TE values (4.89 and 7.35 ms) from which magnitude images and a phase difference map were calculated directly on the scanner. In addition, a high-resolution T1-weighted anatomical image (1 mm isotropic resolution) was obtained for each subject via a three-dimensional (3D) magnetization prepared rapid acquisition of gradient echoes (MP-RAGE) sequence (Mugler 3rd & Brookeman, 1991) with the parameters TR = 2,200 ms, TE = 3.93 ms, flip angle = 9°, TI = 900 ms, FOV = 256×256 mm², single slab with 160 sagittal slices of 1 mm thickness, employing generalized auto-calibrating partially parallel acquisitions (GRAPPA [Griswold et al., 2002]) with an acceleration factor of 2 in phase-encoding direction, yielding a duration of 4 min.

2.4 | Data analysis

Data were analyzed using software packages based on R (version 3.6.1 for Linux; <http://CRAN.R-project.org/> [R Development Core Team, 2008]) and Matlab (version 9.6.0.1150989 for 64-bit Linux, MathWorks, Natick, MS), running on an Intel Core i9® computer (operating system: Ubuntu Linux 18.04.3 64-bit).

2.4.1 | Analysis of the stimulus ratings

A correlation of the ratings of the sensations evoked by the stimuli with the physical strength of the stimuli is a primary requirement in an experimental pain model (Beecher, 1953; Beecher, 1957). The VAS ratings were analyzed with respect to their correlation with the physical strength of the nociceptive stimuli. Values of Spearman's ρ (Spearman, 1904) were calculated separately for each subject and experimental condition. Subsequently, the correlation coefficients were assessed for clusters as a basis for excluding subjects whose ratings were consistently not correlated with stimulus strength, which would violate a basic criterion of experimental pain models (Beecher, 1957). Specifically, following multiplication of the correlation coefficients obtained for the ratings of pleasantness with a value of -1 to obtain uniformly directed coefficients, hierarchical clustering using the Ward algorithm (Ward Jr, 1963) was applied. These analyses were performed using the R library “cluster” (<https://cran.r-project.org/package=cluster> [Maechler, Rousseeuw, Struyf, Hubert, & Hornik, 2019]).

2.4.2 | Assessment of the stimulus-associated brain activations

The processing of the brain images was performed using the statistical parametric mapping toolbox “SPM12” written in Matlab (build 7,487, <https://www.fil.ion.ucl.ac.uk/spm/software/spm12/> [Friston et al., 1995]).

Image preprocessing

Functional MRI image preprocessing included the removal of the first five volumes in the scan series to avert T1 equilibration

effects, realignment of all volumes to the first volume to correct for subject motion, and unwarping on the basis of a static magnetic field map derived from the GE phase data. Subsequently, data were corrected for acquisition time (slice timing). The high-resolution T1-weighted anatomical image was co-registered to the mean EPI (created during the realign and unwarp process), segmented, and normalized using 4th-degree B-spline interpolation to obtain image voxel sizes of $3 \times 3 \times 3 \text{ mm}^3$. The EPI volumes were normalized by applying the resulting spatial normalization parameters and subsequently smoothed with an isotropic 9 mm full-width-half-maximum (FWHM) Gaussian kernel.

Single subject analysis of stimulus-associated brain activations

In an SPM first level single subject analysis, the brain activations following administration of the nociceptive trigeminal CO₂ stimuli were modeled as single regressor in a design matrix. Pain stimuli were modeled as (a) separate delta functions ("stimulus regressor") and convolved with the standard canonical hemodynamic response function (HRF) as provided in SPM12. A first-order parametric regressor (b) was added to modulate the stick function with respect to the "stimulus strength" (CO₂ concentration). The blank stimuli were separately modeled within the design matrix and omitted from second level analysis. Furthermore, the presentation of the VAS, the motoric activity during stimulus rating and the six rotational and translational parameters from the rigid body transformation obtained during image realignment, were modeled as regressors or covariates of no interest. All regressors were convolved with the canonical HRF. Low frequency fluctuations of the MR signal were removed with a high-pass filter with a cut-off at 128 s. Voxelwise regression coefficients for all regressors were estimated using the least squares within SPM12.

After model estimation, the effects of interest were assessed using linear contrasts generating statistical parametric maps of t-values for each subject. The design of this analysis was chosen in accordance with the focus of the analysis of the pain ratings and addressed brain regions where the activations differed with the different strengths of the CO₂ stimuli. Contrast images were created separately for each experimental condition, providing the t-contrast [1] on the first-order parametric CO₂ concentration regressor. These contrast images were generated in a first level analysis and submitted to a group-level analysis.

Group level analysis of stimulus-associated brain activations

The group-level analysis employed a factorial 2×2 analysis of variance (ANOVA) with the factors "stimulation paradigm," that is, the "distinct stimuli" or the "non-distinct stimuli" experimental conditions, and "correlation group," that is, a cluster with high correlation coefficients between stimulus ratings and stimulus strength or a cluster characterized by low correlation coefficients. Contrasts were calculated for (a) the stimulus strength related brain activations across all subjects and experimental conditions (contrast [1 1 1 1]) for "distinct stimuli, correlating group," "distinct stimuli, non-correlating group," "non-distinct stimuli, correlating group," "non-distinct stimuli,

non-correlating group"), (b) greater brain activations during the "distinct stimuli" condition (contrast [1 1 -1 -1]), (c) smaller brain activations during the "distinct stimuli" condition (contrast [-1 -1 1 1]), (d) greater brain activations in the "correlating group" (contrast [1 -1 1 -1]), (e) smaller brain activations in the "correlating group" (contrast [-1 1 -1 1]), and (f) stimulus strength correlated brain activations only in the "correlating group" (contrast [1 0 1 0]) or only in the "non-correlating" group (contrast [0 1 0 1]). The resulting parametric maps of t-statistics were interpreted regarding the probabilistic behavior of Gaussian random fields (Friston, Ashburner, Kiebel, Nichols, & Penny, 2007). If not indicated otherwise, results are reported at a Family Wise Error (FWE [Loring et al., 2002]) corrected α level. A cluster size threshold of five voxels was set. The localization of brain activation was aided by the "Automatic Anatomical Labelling" toolbox (Tzourio-Mazoyer et al., 2002). Significant peak activations were reported as Montreal Neurological Institute (MNI) coordinates, specifying the distance from the anterior commissure in x (right to left), y (anterior to posterior), and z (top to bottom) directions.

Region of interest analysis

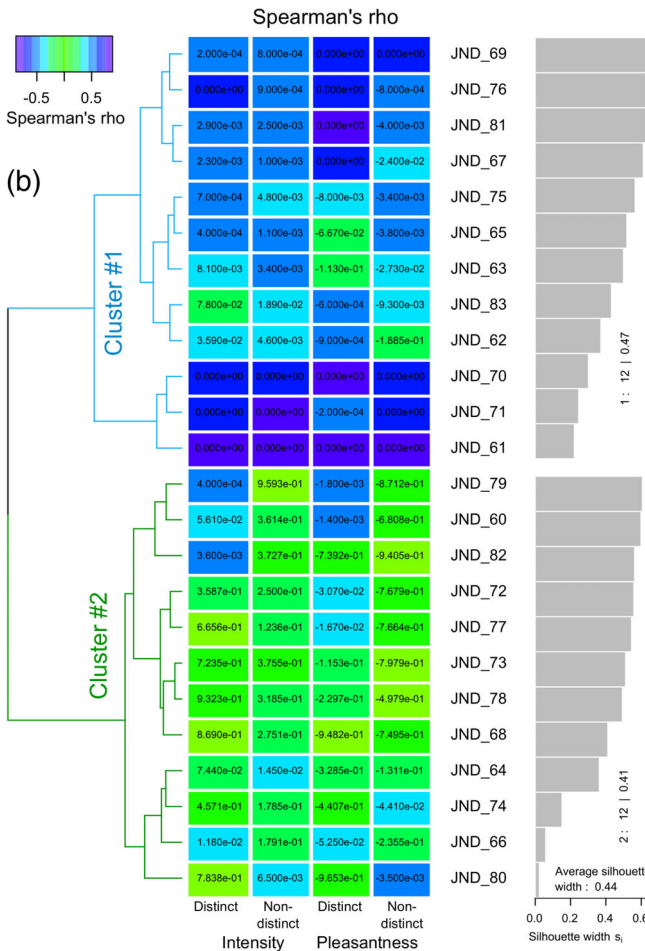
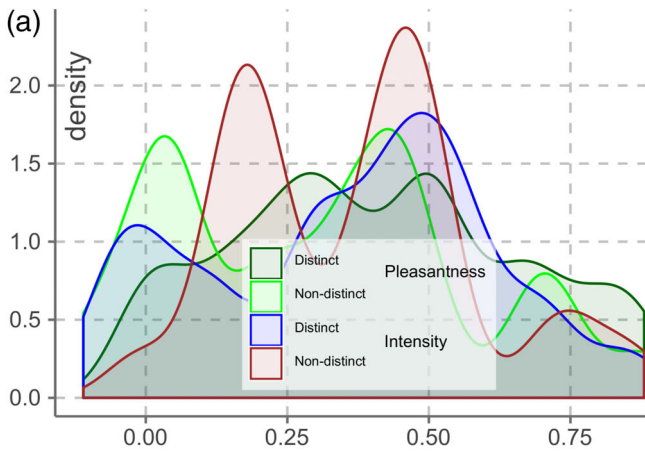
Two brain regions were selected for detailed analysis of association of activations with the stimulus intensity. These included (a) the secondary somatosensory areas S2, based on an earlier association with stimulus intensity coding (Oertel et al., 2012) and on an early magnetoencephalographic study result that localized the main generator of cerebral potentials evoked by the same CO₂ stimuli in S2 (Huttunen, Kobal, Kaukoranta, & Hari, 1986). In addition, the (b) piriform cortex was selected because it was repeatedly involved in encoding chemosensory trigeminal stimuli and study results indicated that this region is important for differences between trigeminal and other nociceptive stimuli (Boyle, Heinke, Gerber, Frasnelli, & Hummel, 2007; Hummel et al., 2009).

Region of interest (ROI) analyses were carried out with the "marsbar" toolbox for SPM (Brett, Anton, Valabregue, & Poline, 2002). Spheres of 10 mm diameter were constructed around the peak coordinates of the ROI. The MNI coordinates were obtained from previous reports. In detail, following right-sided intranasal stimulation S2 had been observed at the MNI coordinates $x = 57$, $y = -6$, $z = 24$ mm and the piriform cortex can be localized at $x = 24$, $y = 4$, $z = -18$ mm (Boyle et al., 2007). For the ROI analyses, the main SPM design estimated in the global analysis was used. The estimated data were extracted and the SPM model subsequently re-estimated. The contrasts of interest were imported from the main analysis, consisting of (a) the stimulus strength related brain activations across all subjects and experimental conditions (contrast [1 1 1 1]) for "different stimuli, correlating group," "different stimuli, non-correlating group," "different stimuli, correlating group," "not different stimuli, correlating group," "not different stimuli, non-correlating group," and (b) larger brain activations in the "correlating group" (contrast [1 -1 1 -1]). In addition, the contrasts [1 0 1 0] and [0 1 0 1] were analyzed to investigate whether piriform activation was also detectable exclusively for the "correlating group" or for the "non-correlating group," respectively.

3 | RESULTS

3.1 | Participants and descriptive data

The 24 subjects included in the study completed the data acquisition. The cohort comprised 12 men and 12 women, aged 22.4–47.1 years (mean ± SD: 27.2 ± 5 years). All subjects had a normal body mass index (22.8 ± 1.6 kg/m²). This provided an initial data set comprising VAS based ratings of the intensity of pain evoked by the nociceptive stimuli and their perceived pleasantness, and full sets of fMRI images acquired during the experiments.



3.2 | Main results

3.2.1 | VAS based stimulus ratings

Pain and pleasantness ratings correlated significantly with the stimulus strength in the majority of 11 subjects. Thus, it was possible to group subjects based on correlation strength (Figure 1). Specifically, hierarchical clustering of the correlation coefficients resulted in two distinct groups of subjects, separating cluster #1 (“strong correlation”) initially comprising $n = 12$ subjects, for whom the VAS ratings correlated with the CO₂ concentration, from cluster #2 (“weak correlation”) comprising $n = 12$ subjects, for whom the correlations were weak. From the strong correlation group with, one subject was excluded as he had rated more than half of the stimuli as zero, which provided a subgroup of $n = 11$ subjects (6 men) in whom stimulus strength and evoked sensations correlated well. The correlations between the VAS ratings of pain intensity evoked by the nociceptive CO₂ stimuli were positively correlated with the CO₂ concentration. In contrast, VAS ratings of the pleasantness of the nociceptive CO₂ stimuli were negatively correlated with the CO₂ concentration (Figure 2).

3.2.2 | Stimulus-associated brain activations

In the $n = 23$ analyzed subjects, areas showing a linear relationship between brain activation and stimulus strength were identified via SPM first level analysis with a t -contrast [1] on the first-order parametric CO₂ concentration regressor. Second level full factorial analysis of the linear relationship between stimulus strength and associated brain activation across both experimental conditions, using the contrast [1 1 1 1] (referring to “distinct stimuli,

FIGURE 1 Group structure ($n = 24$) found among subjects with respect to the correlation between either the VAS ratings of the evoked pain intensity or the pleasantness of the nociceptive CO₂ stimuli with the physical strength of stimuli, given as the CO₂ concentration. (a) Distribution of Spearman's ρ values for both correlations (VAS rating of pain vs. stimuli strength); VAS rating of pleasantness vs. stimuli strength) and both paradigms (distinct stimuli; non-distinct stimuli). The probability density functions suggest multimodality indicating subgroups. (b) The color coding of the heat plot indicates the correlation coefficients. p -values are shown as numbers in the respective cells. For clustering, the correlation coefficients for the pleasantness ratings were multiplied by -1 to obtain uniformly directed correlation data. The dendrogram shows the results of hierarchical cluster analysis (Ward Jr, 1963) of the correlation coefficients. To the right of the heat plot, the Silhouette plot (Rousseeuw, 1987) of the obtained two-cluster solution is shown. The figure has been created using the R software package (version 3.6.1 for Linux; <http://CRAN.R-project.org/> [R Development Core Team, 2008]) and the R packages “gplots” (<https://cran.r-project.org/package=gplots> [Warnes et al., 2020]) and “ggplot2” (<https://cran.r-project.org/package=ggplot2> [Wickham, 2016])

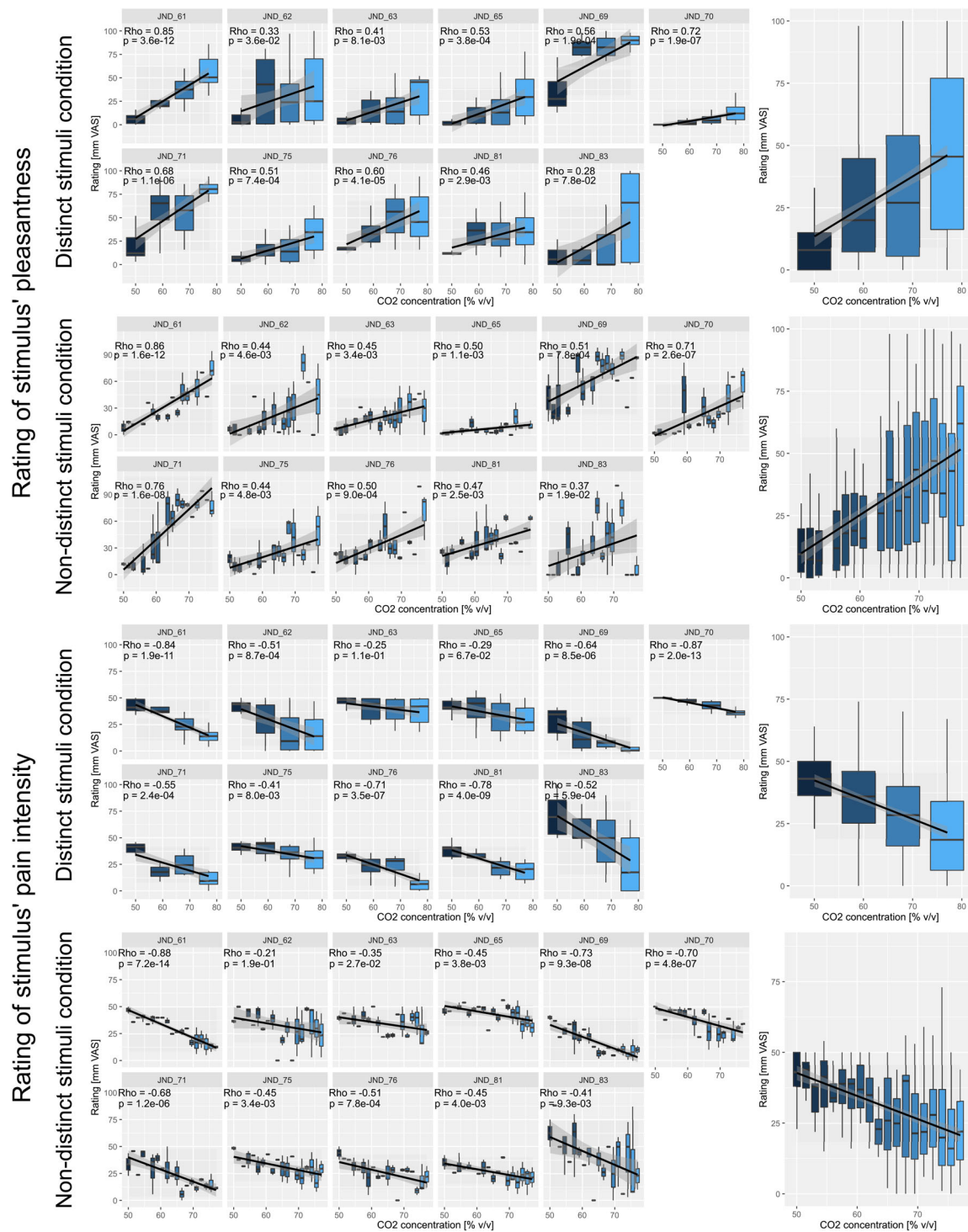


FIGURE 2 Correlations between the ratings of pain evoked by the CO₂ stimuli with respect to pain intensity (top two panels) and stimulus' pleasantness (bottom two panels) in the subjects belonging to cluster #1 ("strong correlation"; $n = 11$, see Figure 1). The values of Spearman's ρ and the corresponding p -values of correlation analysis are displayed for each subject and experimental condition. The ratings were acquired during the "distinct classes stimuli" condition where the 40 stimuli comprised four different strengths (50, 59, 68, and 77% vol/vol CO₂, $n = 10$ each) and again during the "non-distinct classes stimuli" condition (bottom panel) where the 40 stimuli comprised 19 different strengths between 50 and 77% vol/vol at concentration intervals of 1.5% vol/vol. The figure has been created using the R software package (version 3.6.1 for Linux; <http://CRAN.R-project.org/> [R Development Core Team, 2008]) and the library "ggplot2" (<https://cran.r-project.org/package=ggplot2> [Wickham, 2016])

correlating group," "distinct stimuli, non-correlating group," "non-distinct stimuli, correlating group," "non-distinct stimuli, non-correlating group,") identified 11 clusters of activated voxels

(Table 1), using a minimum cluster size of 5 voxels. The largest cluster comprising 353 voxels was located at peak MNI coordinates $x = 48$, $y = -1$, $z = 13$ mm (Figure 3), located in the right Rolandic

Cluster	Coordinates ^a			Label ^b	Distance	T value	P peak level (FWE)
	X	Y	Z				
1	-24	11	-23	Frontal_Inf_Orb_L	0.00	8.21	0.000
	-39	11	-8	Insula_L	0.00	6.70	0.001
	-30	17	-20	Insula_L	0.00	6.56	0.001
2	48	-1	13	Rolandic_Oper_R	0.00	7.74	0.000
	63	2	4	Temporal_Sup_R	0.00	7.53	0.000
	42	-7	13	Rolandic_Oper_R	0.00	7.20	0.000
3	-54	-7	7	Rolandic_Oper_L	0.00	7.40	0.000
4	-42	-13	40	Postcentral_L	0.00	7.17	0.000
	-42	-22	58	Postcentral_L	0.00	6.51	0.001
	-33	-22	46	Postcentral_L	0.00	5.92	0.006
5	36	2	-14	Insula_R	4.00	7.17	0.000
	39	11	-8	Insula_R	0.00	6.93	0.000
6	-6	-28	-8	Lingual_L	6.00	6.84	0.000
	6	-28	-8	Lingual_R	7.87	6.28	0.002
	-12	-22	-8	Hippocampus_L	0.00	6.75	0.002
7	-3	20	28	Cingulum_Ant_L	0.00	6.46	0.000
	6	26	19	Cingulum_Ant_R	0.00	6.05	0.000
8	-36	-13	16	Insula_L	0.00	6.35	0.003
9	-3	-10	43	Cingulum_Mid_L	0.00	6.11	0.003
10	48	32	-8	Frontal_Inf_Orb_R	0.00	5.98	0.004
11	33	-58	-26	Cerebellum_6_R	0.00	5.88	0.005

Note: The group-level analysis ($n = 23$) employed a factorial 2×2 ANOVA with the factors "stimulation paradigm" (i.e., the "distinct stimuli" or the "non-distinct stimuli" experimental conditions) and "correlation group" (according to strong or weak correlations of stimulus ratings with stimulus strength). Contrasts were calculated for (a) the stimulus strength related brain activations across all subjects and experimental conditions (contrast [1 1 1 1], referring to "distinct stimuli, correlating group," "distinct stimuli, non-correlating group," "non-distinct stimuli, correlating group," "non-distinct stimuli, non-correlating group"). The minimum cluster size was set at 5 voxels. Results are reported at the FWE corrected $p < .01$ significance level. For anatomical localization, the "Automatic Anatomical Labelling" toolbox (Tzourio-Mazoyer et al., 2002) was used. Significant peak activations are reported as Montreal Neurological Institute (MNI) coordinates (mm).

^aMNI coordinates.

^bR = right, L = left.

operculum (corresponding to S2). The global maximum activation was observed in a smaller cluster comprising 81 voxels and located at peak MNI coordinates $x = -24$, $y = 11$, $z = -23$ mm (Figure 3), which corresponded to the left inferior frontal orbital lobe. Further activations were observed in the insula, anterior cingulum, the postcentral gyrus, and others, mostly at both sides. Reported results were statistically significant at the FWE corrected level at $p < .01$. A lack of significant brain activations in the [1 1-1 -1] and [-1-1 1 1] contrasts (FWE corrected, $p < .05$) indicated that the increases of brain activation with increasing stimulus strength were similar for the "distinct stimuli" and "non-distinct stimuli" experimental conditions.

Observed subgroups were further explored (Table 2). The contrast [1 0 1 0] (which investigates the "distinct stimuli" and "non-distinct stimuli" experimental conditions exclusively for the

TABLE 1 Brain regions showing a linear relationship between brain activation and stimulus strength, modeled during the SPM first level analysis with a t-contrast [1] on the first-order parametric CO₂ concentration regressor

correlating subgroup) identified eight clusters where brain activations increased significantly with increasing stimulus strength (Table 2). The global maximum activation was observed at MNI coordinates $x = 48$, $y = -4$, $z = 13$ mm (Figure 3), located in the right Rolandic operculum. Larger activations for the correlating than for the non-correlating subgroup (contrast [1-1 1-1]) were observed only at the uncorrected $p < .001$ level (Table 3). For this contrast, seven different clusters were identified; however, the global maximum was located in the left Rolandic operculum at MNI coordinates $x = -51$, $y = -4$, $z = 7$ mm (Figure 4), followed by an activation peak at the right Rolandic operculum at $x = 48$, $y = -4$, $z = 13$ mm. In comparison, the opposite contrast resulted in an "empty brain," that is, no regions were identified which showed more activations in the non-correlating than in the correlating subgroup at an uncorrected $p < .001$.

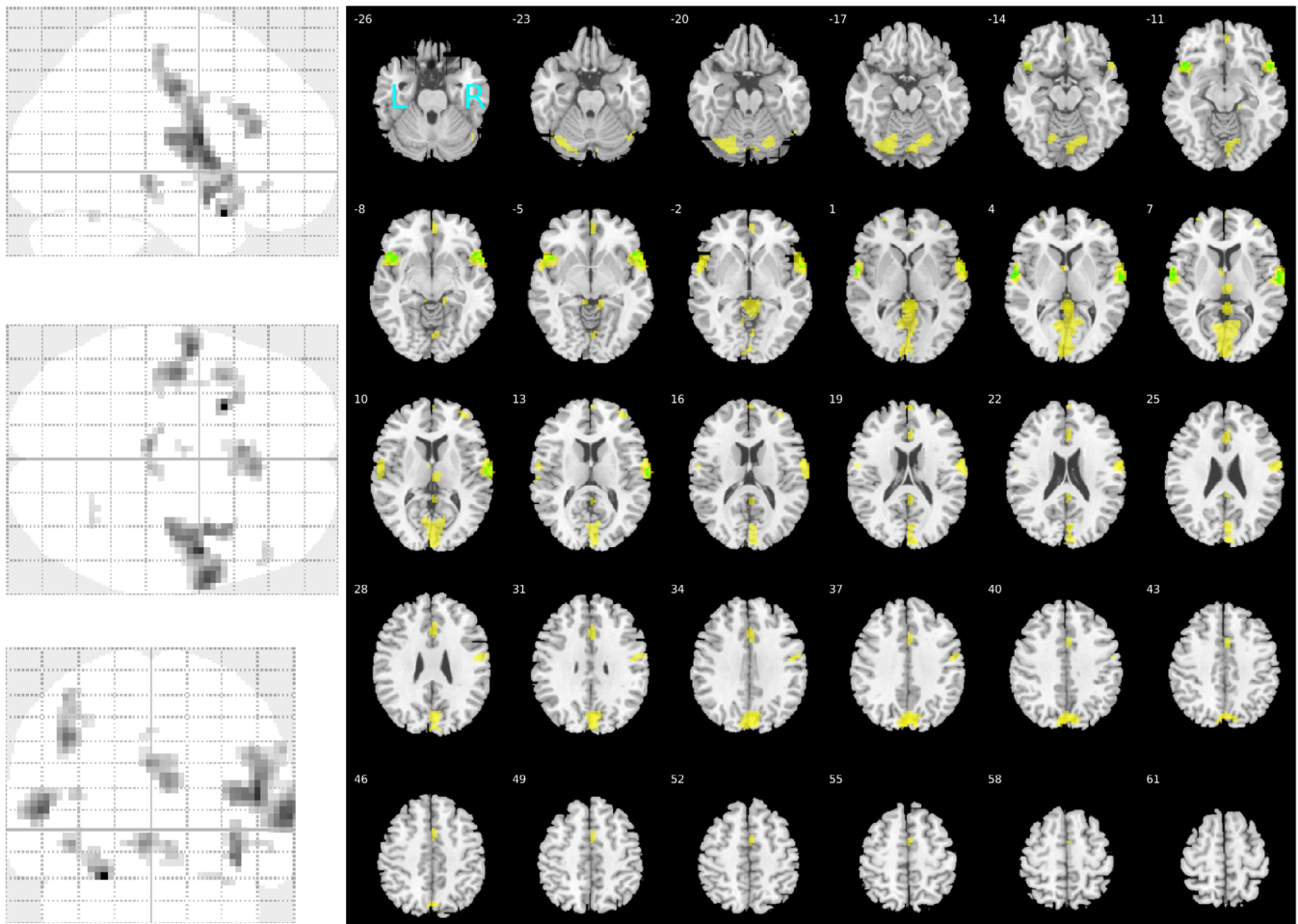


FIGURE 3 Brain regions with significant activations reflecting the linear relationship to the stimulus strength, modeled during the SPM first level analysis with a t -contrast [1] on the first-order parametric CO_2 concentration regressor. Second level full-factorial analysis of the linear relationship between stimulus strength and associated brain activation across both experimental conditions acquired in $n = 23$ subjects. The images show the contrast [1 1 1 1] (referring to “distinct stimuli, correlating group”, “distinct stimuli, non-correlating group”, “non-distinct stimuli, correlating group”, “non-distinct stimuli, non-correlating group”). The results of a t test are shown as a glass brain representation (left) and superimposed on axial slices of the canonical MR template implemented in SPM12 (right). Activations in the $n = 23$ subjects are shown at a threshold of $p < .01$ (FWE-corrected, yellow spots). The minimum cluster size was set at 5 voxels. The activations in the $n = 11$ subjects in whom ratings and stimulus strength were significantly correlated are superimposed as green spots (contrast 1 0 1 0). The figure was created using the SPM12 Matlab toolbox (<http://www.fil.ion.ucl.ac.uk/spm/software/spm12/>; Wellcome Department of Imaging Neuroscience, London, UK [Friston et al., 1995; Worsley & Friston, 1995]) and the xjView Matlab toolbox (version 9.7, <http://www.alivelearn.net/xjview>)

3.3 | Results of regions of interest analyses

The stimulus strength linked activation patterns in S2, located from previous reports (Boyle et al., 2007) at MNI coordinates $x = 57$, $y = -6$, $z = 24$ mm, repeated the findings in the main analyses. Both contrasts [1 1 1 1] and [1-1 1-1] were statistically significant reflecting stimulus intensity dependent activations in both subgroups but larger in the correlating than for the non-correlating subgroup (Table 4). The piriform cortex, located from previous reports (Boyle et al., 2007) at MNI coordinates at $x = 24$, $y = 4$, $z = -18$ mm, showed similar activations, however, at lower statistical significance than at S2. It is noteworthy that when the comparative analyses were skipped and only the activations exclusively for the “correlating group” (contrast [1 0 1 0]) or for the “non-correlating group” (contrast [0 1 0 1])

were evaluated, statistically significant activations in the piriform cortex were found only in the “correlating group” (Table 4).

4 | DISCUSSION

By applying a well-established experimental human pain model using a chemical trigeminal stimulus, the present study investigated brain areas that are currently assumed to be activated in a pain stimulus-strength dependent manner. The results point at the secondary somatosensory cortex S2 as the brain area predominantly involved in the subjective perception of different pain stimulus intensities. This result was obtained by using two distinct stimulation paradigms, which proved to be equivalent. This indicates that future experiments on testing analgesic drug

Cluster	Coordinates ^a			Label ^b	Distance	T value	P peak level (FWE)
	X	Y	Z				
1	48	-4	13	Rolandic_Oper_R	0.00	7.16	0.000
	42	-13	16	Rolandic_Oper_R	0.00	6.50	0.001
2	-51	-7	7	Rolandic_Oper_L	0.00	6.84	0.000
3	36	2	-14	Insula_R	4.00	6.35	0.002
4	36	14	-5	Insula_R	1.00	6.15	0.003
5	-42	-13	40	Postcentral_L	0.00	6.05	0.004
6	63	-1	7	Rolandic_Oper_R	0.00	6.02	0.004
7	-39	20	-11	Frontal_Inf_Orb_L	0.00	5.99	0.005
8	69	-16	16	Postcentral_R	0.00	5.90	0.006
	63	-16	10	Temporal_Sup_R	0.00	5.83	0.007

Note: The group-level analysis employed a factorial 2 × 2 ANOVA with the factors “stimulation paradigm” (i.e., the “distinct stimuli” or the “non-distinct stimuli” experimental conditions) and “correlation group” (i.e., groups of subjects based on strong or weak correlations of stimulus ratings with stimulus strength). The contrast [1 0 1 0] is shown, referring to “distinct stimuli, correlating group,” “distinct stimuli, non-correlating group,” “non-distinct stimuli, correlating group,” “non-distinct stimuli, non-correlating group.” The minimum cluster size was set at 5 voxels. Results are reported at the FWE corrected $p < .01$ significance level. For anatomical localization, the “Automatic Anatomical Labelling” toolbox (Tzourio-Mazoyer et al., 2002) was used. Significant peak activations are reported as Montreal Neurological Institute (MNI) coordinates (mm).

^aMNI coordinates.

^bR = right, L = left.

TABLE 2 Brain regions showing a linear relationship between brain activation and stimulus strength in the $n = 11$ subjects for whom ratings and stimulus strength were significantly correlated

Cluster	Coordinates ^a			Label ^b	Distance (mm)	T value	P peak level (uncorrected)
	X	Y	Z				
1	-51	-4	7	Rolandic_Oper_L	0	4.30	0.000
2	48	-4	13	Rolandic_Oper_R	0	4.12	0.000
	42	-13	16	Rolandic_Oper_R	0	3.43	0.001
3	-42	20	-11	Frontal_Inf_Orb_L	0	4.07	0.000
	-33	20	4	Insula_L	0	3.57	0.000
	-51	26	-14	Frontal_Inf_Orb_L	1	3.50	0.001
4	66	-13	10	Temporal_Sup_R	0	3.81	0.000
5	-60	-43	40	Parietal_Inf_L	0	3.78	0.000
	-54	-55	43	Parietal_Inf_L	0	3.37	0.001
6	-30	29	-5	Frontal_Inf_Orb_L	0	3.67	0.000
7	-36	5	10	Insula_R	0	3.54	0.000
8	39	17	-2	Insula_L	0	3.49	0.001

Note: Second level full-factorial analysis of the linear relationship between stimulus strength and associated brain activation across both experimental conditions. The images show the contrast [1-1 1-1] (referring to “distinct stimuli, correlating group,” “distinct stimuli, non-correlating group,” “non-distinct stimuli, correlating group,” “non-distinct stimuli, non-correlating group”). The minimum cluster size was set at 5 voxels. Results are reported at the uncorrected $p < .001$ significance level. For anatomical localization, the “Automatic Anatomical Labelling” toolbox (Tzourio-Mazoyer et al., 2002) was used. Significant peak activations are reported as Montreal Neurological Institute (MNI) coordinates (mm).

^aMNI coordinates.

^bR = right, L = left.

TABLE 3 Brain regions where activations reflecting the linear relationship to the stimulus strength, modeled during the SPM first level analysis with a t-contrast [1] on the first-order parametric CO₂ concentration regressor, were larger for the correlating group than for the non-correlating group

effects can be designed without a preference for either paradigm, that is, using either a few distinct nociceptive stimuli or a larger variety of nociceptive stimuli. As a further result of the present study, the

secondary somatosensory cortex appears to be one of the most promising target areas to observe in analgesic drug research, especially when using trigeminal nociceptive stimulation as the experimental paradigm.

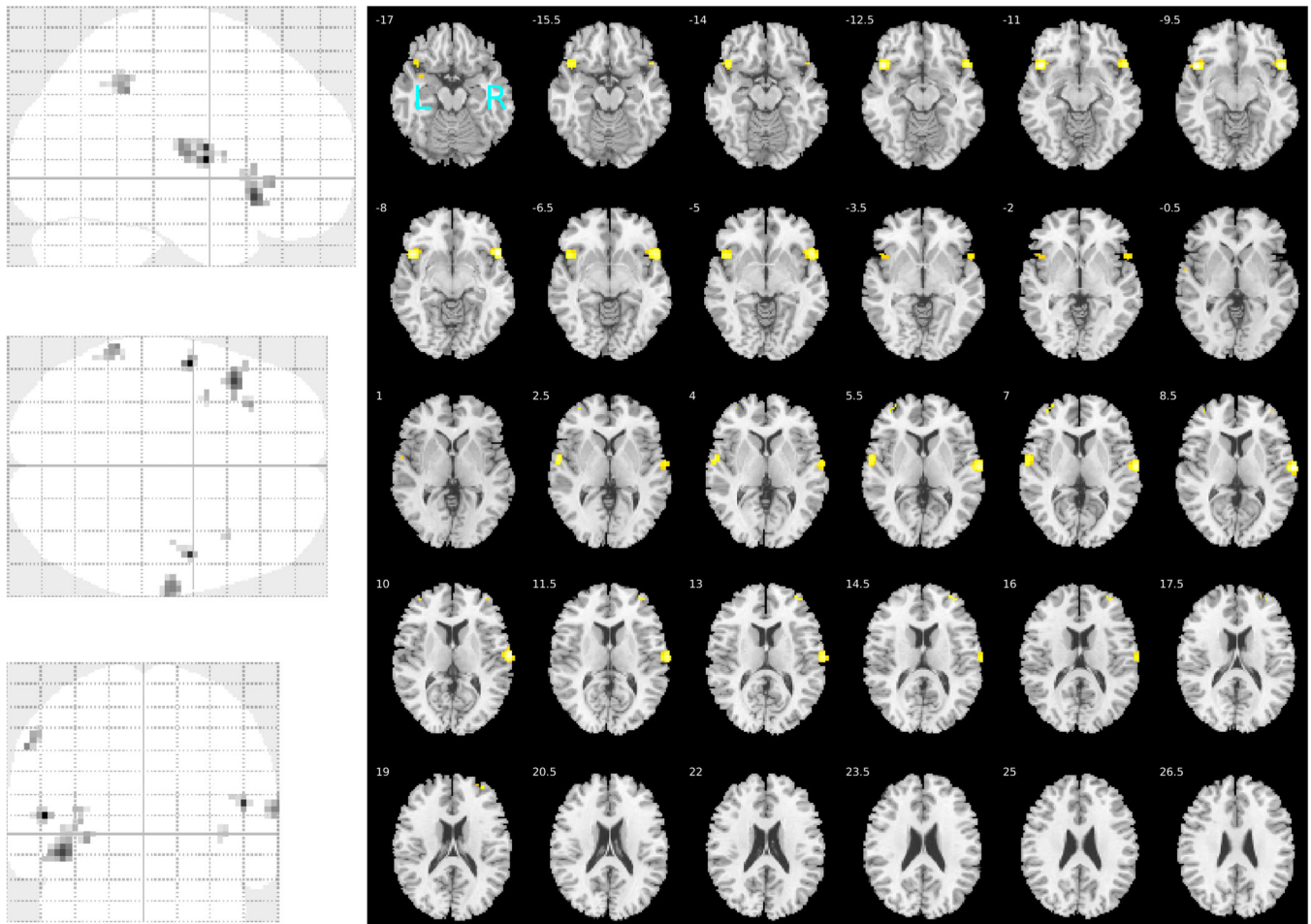


FIGURE 4 Brain regions where activations reflecting the linear relationship to the stimulus strength, modeled during the SPM first level analysis with a t-contrast [1] on the first-order parametric CO₂ concentration regressor, were larger for the correlating than for the non-correlating subgroup. Second level full-factorial analysis of the linear relationship between stimulus strength and associated brain activation across both experimental conditions. The images show the contrast [1 -1 1 -1] (referring to “distinct stimuli, correlating group,” “distinct stimuli, non-correlating group,” “non-distinct stimuli, correlating group,” “non-distinct stimuli, non-correlating group”). The results of a t test are shown as a glass brain representation (left) and superimposed on axial slices of the canonical MR template implemented in SPM12 (right). The significance at voxel level is color coded from light blue to green with increasing t values. Activations are shown at an uncorrected threshold of $p < .001$. The minimum cluster size was set at 5 voxels. The figure was created using the SPM12 Matlab toolbox (<http://www.fil.ion.ucl.ac.uk/spm/software/spm12/>; Wellcome Department of Imaging Neuroscience, London, UK [Friston, Holmes, Poline, et al., 1995; Worsley & Friston, 1995]) and the xjView Matlab toolbox (version 9.7, <http://www.alivelearn.net/xjview>)

The present results indicate that intranasal trigeminal stimulation produces brain activation in areas typically involved in the perception and processing of pain (Lee et al., 2013; Walter et al., 2016) described as “body-self neuromatrix” (Iannetti & Mouraux, 2010). This presently included the thalamus, the insula, the primary and secondary somatosensory cortex, the fronto-orbital cortex and a few further brain regions such as the cerebellum. The results thereby agree with the nociceptive specificity of the gaseous CO₂ stimuli which is further supported by the results of several previous studies, comprising the following findings: Firstly, CO₂ stimuli are known to activate trigeminal A_δ-fibers, with co-activation of C-fibers (Steen et al., 1992). Secondly, subjects are able to identify the stimulated side following unilateral intranasal application, which is impossible with pure olfactory stimuli (Kobal, Van Toller, & Hummel, 1989). Thirdly, CO₂ stimuli

can be perceived by subjects without a functional olfactory system (Frasnelli, Schuster, & Hummel, 2007). Fourthly, CO₂ stimuli are rated as odorless, that is, with zero-intensity of smell (Lötsch et al., 2012).

The location of the presently reported activations is compatible with previous observations that, however, had been found in an experiment that did not assess the stimulus-strength dependency. That is, employing a block design as opposed to the present event-related design, administration of CO₂ stimuli at 60% vol/vol was associated with brain activations at the uncorrected significance level ($p = .001$) that were located in the precentral gyrus, superior temporal sulcus, insula, postcentral gyrus (SI), secondary somatosensory area (S2), cerebellum, ventrolateral thalamus (and other thalamus parts), piriform cortex, orbito-frontal cortex and amygdala (Boyle et al., 2007). Especially the activation of the piriform cortex emphasizes the close connection of

TABLE 4 Results of region of interest analyses assessing the stimulus strength dependent brain activations at the secondary somatosensory area S2 and at the piriform cortex, located at MNI coordinates $x = 57, y = -6, z = 24$ mm (Boyle et al., 2007) and $x = 24, y = 4, z = -18$ mm (Boyle et al., 2007), respectively

Area	Contrast ^a	T value	P peak level (uncorrected)
S2	[1 1 1 1]	5.79	0
	[1-1 1-1]	2.2	0.016517
Piriform cortex	[1 1 1 1]	3.77	0.000255
	[1-1 1-1]	2.05	0.023346
	[1 0 1 0]	3.54	0.000501
	[0 1 0 1]	1.51	0.069532

Note: Contrasts were calculated for (a) the stimulus strength related brain activations across all subjects and experimental conditions (contrast [1 1 1 1], referring to “distinct stimuli, correlating group,” “distinct stimuli, non-correlating group,” “non-distinct stimuli, correlating group,” “non-distinct stimuli, non-correlating group”) and (b) for greater stimulus strength related brain activations for the correlating group than for the non-correlating group (contrast [1-1 1-1]). In addition, the piriform cortex as of major interest was also examined for activations exclusively for the “correlating group” (contrast [1 0 1 0]) or for the “non-correlating group” (contrast [0 1 0 1]).

^aContrasts imported from the main full factorial analysis reported in Tables 1 and 3.

the intranasal trigeminal system to the sense of smell. Because trigeminal sensations like tickling, stinging or burning can be elicited by the majority of odors (Doty et al., 1978) this association is easily explained (Hummel & Frasnelli, 2019).

In contrast to the above-mentioned analysis, further investigations focused on brain responses to nociceptive stimuli that correlated with the physical stimulus strength, given by the concentration of the gaseous CO₂. This analysis was implemented as first level regressor for the CO₂ concentration assigned to the regressor capturing the application of the suprathreshold stimuli. Brain regions identified to be activated in the present experiment by this regressor agree with those that were found in previous experiments to display activations that increase with the stimulus strength. This includes the insula, superior temporal gyrus, S2, amygdala, postcentral gyrus (SI), and parts of the cingulate cortex (Oertel et al., 2012). These areas were identified in a similar manner as in the present assessments to display activations related to stimulus strength, and included again, the insula, the Rolandic operculum (S2), and in addition supramarginal areas, primary and supplementary motor areas, the cingulate cortex, as well as occipital, lingual, temporal, frontal and fusiform parts of the brain (Annak et al., 2018).

To further address the subjective perception of different pain intensities from the degree of their correlation with the stimulus strength, two subgroups of subjects could be separated with either strong or rather weak correlations in the present VAS ratings. Analyzing these data allowed to locate brain areas that showed comparatively more activations in the group where the ratings correlated strongly with the stimulus strength. Although these particular results have to be regarded with caution, considering the low significance level ($p < .001$ uncorrected, however, compare (Boyle et al., 2007) where all results were published

only at an uncorrected p level), the location of activations may point at brain areas directly involved in the conscious perception of the strength of nociceptive stimuli. The analysis pointed once more at the secondary somatosensory cortex as the region where the activation differed most clearly between the subject subgroups. In addition to its previous appearance among regions associated with the coding of stimulus intensity, S2 was the first brain area associated with the nociceptive excitation produced by the CO₂ stimuli. Specifically, in a magnetoencephalographic experiment performed more than 30 years ago, S2 was identified as the location of the source of the neuronal sum potential evoked by the stimuli (Huttunen et al., 1986). Neuroanatomical evidence supports that S2 contributes to the encoding of painful stimuli (Bornhövd et al., 2002). The region receives projections from the dorsomedial thalamus, which itself receives projections from the brain stem trigeminal nuclei (Bowsher, 2005; Craig, 2004).

Further brain regions with comparatively more activation in the subgroup whose ratings correlated with the stimulus strength were the insular cortex and frontal orbital and parietal inferior cortical areas. All these regions have been shown previously to be involved in the encoding of stimulus intensity (Oertel et al., 2012). The posterior insula has been frequently reported as a major localization of pain-related brain activation and intensity encoding (Boly et al., 2007; Bornhövd et al., 2002; Casey et al., 1994; Coghill et al., 1994; Coghill, Sang, Maisog, & Iadarola, 1999; Derbyshire et al., 1997; Talbot et al., 1991; Tölle et al., 1999). It has extensive connections with other brain regions such as the prefrontal cortex, cingulate cortex, amygdala, parahippocampal gyrus, and secondary somatosensory cortex (Friedman & Murray, 1986; Friedman, Murray, O'Neill, & Mishkin, 1986; Mesulam & Mufson, 1982; Mufson & Mesulam, 1982; Mufson, Mesulam, & Pandya, 1981) and may therefore act as an integrative structure for various information about the stimulus, working memory, affect, attention, and others (Starr et al., 2009). Indeed, the relation between stimulus strength and intensity of the evoked pain is subject to many modulatory influences, such as hedonic properties of the stimuli (Wiech et al., 2010), arousal (Ring, Kavussanu, & Willoughby, 2013), expectations (Keltner et al., 2006), attention bias (Tracey et al., 2002), reward (Navratilova & Porreca, 2014) and others. Further evidence for the importance of the insula as a key area in this pain context are reports of patients with lesions of the posterior insula, who exhibited elevated pain thresholds (Greenspan, Lee, & Lenz, 1999; Greenspan & Winfield, 1992). Moreover, pain could be induced only by electrical stimulation of the insula in the absence of physical pain model (Mazzola, Isnard, Peyron, Guenot, & Mauguier, 2009). The frontal inferior orbital cortex is also well-connected to many areas including the somatosensory areas SI, S2 and the insula and has been reported to be involved in a regulatory manner in the subjective and emotional value of stimuli as well as in pain inhibition (Moont, Crispel, Lev, Pud, & Yarnitsky, 2011; Rolls & Grabenhorst, 2008). Interestingly, the orbitofrontal cortex was recently also found to be part of a system contextually ranking and making decisions about pain (Winston, Vlaev, Seymour, Chater, & Dolan, 2014). In contrast, the inferior parietal lobule, together with S1 and S2, is frequently related to the sensory-discriminative aspects of painful stimuli, rather than the affective processing, and plays a major role in the conscious experience of pain (Albanese & Duncan, 2007).

4.1 | Strengths and limitations

One subject was excluded from the data analysis because he had evaluated more than half of the CO₂ stimuli as not painful at all. For this purpose, the data quality in the “non-correlating” cluster must be discussed. Zero-ratings of pain intensity may indicate a problem in the instruction of the subjects, that is, since experimental pain is limited in intensity for ethical reasons, subjects may have difficulties in evaluating a stimulus as pain despite careful instruction during the mandatory training session, or technical problems may occur in the delivery of stimuli. The latter may occasionally occur with chemosensory stimuli if the subject exhales through the nose at the exact moment when the gaseous stimulus is administered intranasally. Therefore, subjects learn a special breathing technique called “velopharyngeal closure” (Huttunen et al., 1986; Kobal, 1985), but it is possible that this technique is not maintained during the test session. However, zero evaluations of intentionally supra-threshold CO₂ stimuli are not specific to the present data set, but commonly recorded in similar studies. In extreme cases, when only the presence of a ceiling effect was investigated and CO₂ stimuli are administered in concentrations of up to 100%, about 5% of healthy subjects

did not reliably perceive a stimulus of 2000 ms of pure CO₂ (Hummel, Kaehling, & Grosse, 2016). Nevertheless, the central tendency of the present ratings was unsuspecting up to almost ideally reflecting a linear concentration versus response relationship (Figure 2), and when used as an experimental human pain model, CO₂ stimuli figure among the best predictors of effects of analgesic drugs on clinical pain (Lötsch et al., 2014; Oertel & Lotsch, 2013).

To further conclude that non-correlation between stimulus ratings and strength and occasional ratings of zero pain intensity were not indicative of technical problems leading to failure of stimulus delivery, a separate SPM second level group analysis was conducted in the same way as the main analysis, but using the regressor in the design matrix used to model the CO₂ stimuli, rather than the regressor that coded for their strength. Contrasts were calculated (a) for stimulus-related brain activations only in the “correlating group” (contrast [1 0 1 0]) and (b) only in the “non-correlating group” (contrast [0 1 0 1]). The results confirmed that stimulus-associated brain activations were present in both subgroups (Figure 5), whereby, as expected, more activations were present in the correlating group, but certainly also in the non-correlating group. This suggests that the

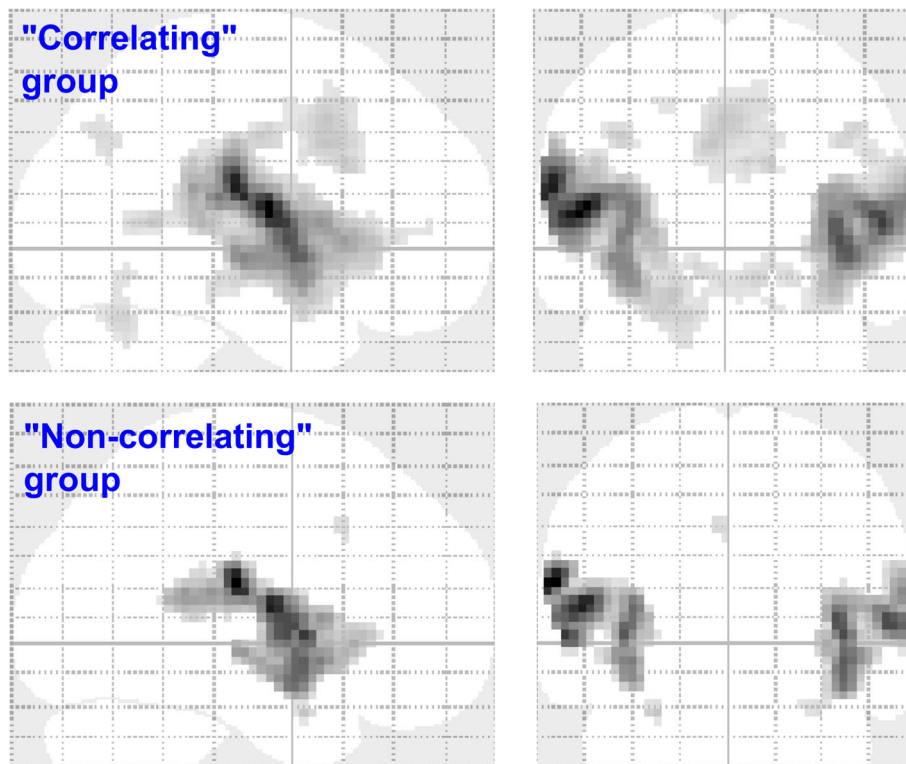


FIGURE 5 Brain regions with significant activations associated with the nociceptive CO₂ stimuli regardless of their concentration > 0%. The figure shows the result of a separate second level analysis of the contrast on the regressor coding in the first level a design matrix for the administration of the nociceptive trigeminal CO₂ stimuli as separate delta functions (“stimulus regressor”). Subsequently, a second level analysis was performed analogously as for the stimulus strength related analyses, employing a factorial 2 × 2 ANOVA with the factors “stimulation paradigm” and “correlation group.” The images show the contrast [1 0 1 0] (i.e., activations in the “correlating group”) during both the “distinct stimuli” and the “non-distinct stimuli” condition (upper row) and the contrast [0 1 0 1] (i.e., activations in the “non-correlating group”) during both the “distinct stimuli” and the “non-distinct stimuli” condition (lower row). The figure was created using the SPM12 Matlab toolbox (<http://www.fil.ion.ucl.ac.uk/spm/software/spm12/>; Wellcome Department of Imaging Neuroscience, London, UK [Friston, Holmes, Poline, et al., 1995; Worsley & Friston, 1995])

available findings on subgroup differences are not due to poor data quality due to technical problems in the nonsupply of CO₂ stimuli.

5 | CONCLUSIONS

Results of the present study support previous findings (Huttunen et al., 1986; Oertel et al., 2012) that suggest a major role of the secondary somatosensory cortex in coding the subjectively perceived intensity of intranasal trigeminal stimuli. Importantly, the results also support the piriform cortex, in addition to the secondary somatosensory cortex, as a major area of interest for stimulus strength-related brain activation in pain models using trigeminal stimuli. This makes both areas a primary objective to be observed in human experimental pain settings where trigeminal input is used to study effects of analgesics.

ACKNOWLEDGEMENT

Open access funding enabled and organized by Projekt DEAL.

[Correction added on 26 September 2020, after first online publication: Projekt Deal funding statement has been added.]

CONFLICT OF INTEREST

The authors have declared that no competing interests exist.

DATA AVAILABILITY STATEMENT

The original data are available from the first author on request.

ORCID

Jörn Lötsch  <https://orcid.org/0000-0002-5818-6958>

REFERENCES

- Albanese, M.-C., & Duncan, G. (2007). PET and fMRI imaging in parietal cortex (SI, SII, inferior parietal cortex BA40). In R. F. Schmidt & W. D. Willis (Eds.), *Encyclopedia of pain* (pp. 1809–1810). Berlin, Heidelberg: Springer Berlin Heidelberg.
- Albrecht, J., Kopietz, R., Frasnelli, J., Wiesmann, M., Hummel, T., & Lundström, J. N. (2010). The neuronal correlates of intranasal trigeminal function—an ALE meta-analysis of human functional brain imaging data. *Brain Research Reviews*, *62*, 183–196.
- Andersson, J. L., Hutton, C., Ashburner, J., Turner, R., & Friston, K. (2001). Modeling geometric deformations in EPI time series. *NeuroImage*, *13*, 903–919.
- Annak, O., Heidegger, T., Walter, C., Deichmann, R., Nöth, U., Hansen-Goos, O., ... Lötsch, J. (2018). Effects of continuous theta-burst stimulation of the primary motor and secondary somatosensory areas on the central processing and the perception of trigeminal nociceptive input in healthy volunteers. *Pain*, *160*(1), 172–186.
- Anton, F., Euchner, I., & Handwerker, H. (1992). Psychophysical examination of pain induced by defined CO₂ pulses applied to the nasal mucosa. *Pain*, *49*, 53–60.
- Beecher, H. K. (1953). Limiting factors in experimental pain. *Journal of Chronic Diseases*, *4*, 11–26.
- Beecher, H. K. (1957). The measurement of pain: Prototype for the quantitative study of subjective responses. *Pharmacological Reviews*, *9*, 59–209.
- Bingel, U., & Tracey, I. (2008). Imaging CNS modulation of pain in humans. *Physiology*, *23*, 371–380.
- Boly, M., Balteau, E., Schnakers, C., Degueldre, C., Moonen, G., Luxen, A., ... Laureys, S. (2007). Baseline brain activity fluctuations predict somatosensory perception in humans. *Proceedings of the National Academy of Sciences of the United States of America*, *104*, 12187–12192.
- Bornhövd, K., Quante, M., Glauche, V., Bromm, B., Weiller, C., & Büchel, C. (2002). Painful stimuli evoke different stimulus-response functions in the amygdala, prefrontal, insula and somatosensory cortex: A single-trial fMRI study. *Brain*, *125*, 1326–1336.
- Bowsher, D. (2005). Representation of somatosensory modalities in pathways ascending from the spinal anterolateral funiculus to the thalamus demonstrated by lesions in man. *European Neurology*, *54*, 14–22.
- Boyle, J. A., Heinke, M., Gerber, J., Frasnelli, J., & Hummel, T. (2007). Cerebral activation to intranasal chemosensory trigeminal stimulation. *Chemical Senses*, *32*, 343–353.
- Brett, M., Anton, J.L., Valabregue, R., Poline, J.B. (2002) Region of interest analysis using an SPM toolbox. Paper presented at 8th International Conference on Functional Mapping of the Human Brain. Sendai, Japan.
- Casey, K. L., Minoshima, S., Berger, K. L., Koeppe, R. A., Morrow, T. J., & Frey, K. A. (1994). Positron emission tomographic analysis of cerebral structures activated specifically by repetitive noxious heat stimuli. *Journal of Neurophysiology*, *71*, 802–807.
- Coghill, R. C., Sang, C. N., Maisog, J. M., & Iadarola, M. J. (1999). Pain intensity processing within the human brain: A bilateral, distributed mechanism. *Journal of Neurophysiology*, *82*, 1934–1943.
- Coghill, R. C., Talbot, J. D., Evans, A. C., Meyer, E., Gjedde, A., Bushnell, M. C., & Duncan, G. H. (1994). Distributed processing of pain and vibration by the human brain. *The Journal of Neuroscience*, *14*, 4095–4108.
- Craig, A. D. (2004). Distribution of trigeminothalamic and spinothalamic lamina I terminations in the macaque monkey. *The Journal of Comparative Neurology*, *477*, 119–148.
- Derbyshire, S. W., Jones, A. K., Gyulai, F., Clark, S., Townsend, D., & Firestone, L. L. (1997). Pain processing during three levels of noxious stimulation produces differential patterns of central activity. *Pain*, *73*, 431–445.
- Doty, R. L., Brugger, W. E., Jurs, P. C., Orndorff, M. A., Snyder, P. J., & Lowry, L. D. (1978). Intranasal trigeminal stimulation from odorous volatiles: Psychometric responses from anosmic and normal humans. *Physiology & Behavior*, *20*, 175–185.
- Fechner, G.T. (1860) *Elemente der Psychophysik*. Leipzig. Breitkopf and Härtel.
- Frasnelli, J., Schuster, B., & Hummel, T. (2007). Subjects with congenital anosmia have larger peripheral but similar central trigeminal responses. *Cerebral Cortex*, *17*, 370–377.
- Friedman, D. P., & Murray, E. A. (1986). Thalamic connectivity of the second somatosensory area and neighboring somatosensory fields of the lateral sulcus of the macaque. *The Journal of Comparative Neurology*, *252*, 348–373.
- Friedman, D. P., Murray, E. A., O'Neill, J. B., & Mishkin, M. (1986). Cortical connections of the somatosensory fields of the lateral sulcus of macaques: Evidence for a corticolimbic pathway for touch. *The Journal of Comparative Neurology*, *252*, 323–347.
- Friston, K. J., Ashburner, J. T., Kiebel, S. J., Nichols, T. E., & Penny, W. D. (Eds.). (2007). *Statistical parametric mapping, the analysis of functional brain images* (1st ed.). Amsterdam, The Netherlands: Elsevier.
- Friston, K. J., Fletcher, P., Josephs, O., Holmes, A., Rugg, M. D., & Turner, R. (1998). Event-related fMRI: Characterizing differential responses. *NeuroImage*, *7*, 30–40.
- Friston, K. J., Holmes, A. P., Poline, J. B., Grasby, P. J., Williams, S. C., Frackowiak, R. S., & Turner, R. (1995). Analysis of fMRI time-series revisited. *NeuroImage*, *2*, 45–53.
- Friston, K. J., Holmes, A. P., Worsley, K. J., Poline, J. B., Frith, C. D., & Frackowiak, R. S. (1995). Statistical parametric maps in functional imaging: A general linear approach. *Human Brain Mapping*, *2*, 189–210.
- Greenspan, J. D., Lee, R. R., & Lenz, F. A. (1999). Pain sensitivity alterations as a function of lesion location in the parasympathetic cortex. *Pain*, *81*, 273–282.

- Greenspan, J. D., & Winfield, J. A. (1992). Reversible pain and tactile deficits associated with a cerebral tumor compressing the posterior insula and parietal operculum. *Pain*, *50*, 29–39.
- Griswold, M. A., Jakob, P. M., Heidemann, R. M., Nittka, M., Jellus, V., Wang, J., ... Haase, A. (2002). Generalized autocalibrating partially parallel acquisitions (GRAPPA). *Magnetic Resonance in Medicine*, *47*, 1202–1210.
- Handwerker, H., & Kopal, G. (1993). Psychophysiology of experimentally induced pain. *Physiological Reviews*, *73*, 639–671.
- Hummel, T., & Frasnelli, J. (2019). The intranasal trigeminal system. In R. L. Doty (Ed.), *Handbook of clinical neurology*. Amsterdam, The Netherlands: Elsevier.
- Hummel, T., Kaehling, C., & Grosse, F. (2016). Automated assessment of intranasal trigeminal function. *Rhinology*, *54*, 27–31.
- Hummel, T., & Kopal, G. (1999). Chemosensory event-related potentials to trigeminal stimuli change in relation to the interval between repetitive stimulation of the nasal mucosa. *European Archives of Otorhino-Laryngology*, *256*, 16–21.
- Hummel, T., & Livermore, A. (2002). Intranasal chemosensory function of the trigeminal nerve and aspects of its relation to olfaction. *International Archives of Occupational and Environmental Health*, *75*, 305–313.
- Hummel, T., Mohammadian, P., Marchl, R., Kopal, G., & Lötsch, J. (2003). Pain in the trigeminal system: Irritation of the nasal mucosa using short- and long-lasting stimuli. *International Journal of Psychophysiology*, *47*, 147–158.
- Hummel, T., Oehme, L., van den Hoff, J., Gerber, J., Heinke, M., Boyle, J. A., & Beuthien-Baumann, B. (2009). PET-based investigation of cerebral activation following intranasal trigeminal stimulation. *Human Brain Mapping*, *30*, 1100–1104.
- Hutton, C., Bork, A., Josephs, O., Deichmann, R., Ashburner, J., & Turner, R. (2002). Image distortion correction in fMRI: A quantitative evaluation. *NeuroImage*, *16*, 217–240.
- Huttunen, J., Kopal, G., Kaukoranta, E., & Hari, R. (1986). Cortical responses to painful CO₂ stimulation of nasal mucosa: A magnetoencephalographic study in man. *Electroencephalography and Clinical Neurophysiology*, *64*, 347–349.
- Iannetti, G. D., & Mouraux, A. (2010). From the neuromatrix to the pain matrix (and back). *Experimental Brain Research*, *205*, 1–12.
- Keltner, J. R., Furst, A., Fan, C., Redfern, R., Inglis, B., & Fields, H. L. (2006). Isolating the modulatory effect of expectation on pain transmission: A functional magnetic resonance imaging study. *The Journal of Neuroscience*, *26*, 4437–4443.
- Kopal, G. (1981). *Elektrophysiologische Untersuchungen des menschlichen Geruchsinnes*. Stuttgart: Thieme-Verlag.
- Kopal, G. (1985). Pain-related electrical potentials of the human nasal mucosa elicited by chemical stimulation. *Pain*, *22*, 151–163.
- Kopal, G., Van Toller, S., & Hummel, T. (1989). Is there directional smelling? *Experientia*, *45*, 130–132.
- Lee, M. C., Ploner, M., Wiech, K., Bingel, U., Wanigasekera, V., Brooks, J., ... Tracey, I. (2013). Amygdala activity contributes to the dissociative effect of cannabis on pain perception. *Pain*, *154*, 124–134.
- Loring, D. W., Meador, K. J., Allison, J. D., Pillai, J. J., Lavin, T., Lee, G. P., ... Dave, V. (2002). Now you see it, now you don't: Statistical and methodological considerations in fMRI. *Epilepsy & Behavior*, *3*, 539–547.
- Lötsch, J., Oertel, B. G., & Ullsch, A. (2014). Human models of pain for the prediction of clinical analgesia. *Pain*, *155*, 2014–2021.
- Lötsch, J., Walter, C., Felden, L., Noth, U., Deichmann, R., & Oertel, B. G. (2012). The human operculo-insular cortex is pain-preferentially but not pain-exclusively activated by trigeminal and olfactory stimuli. *PLoS ONE*, *7*, e34798.
- Machler, M., Rousseeuw, P., Struyf, A., Hubert, M., & Hornik, K. (2019). Cluster: Cluster Analysis Basics and Extensions. R package version 2.1.0.
- Mazzola, L., Isnard, J., Peyron, R., Guenot, M., & Mauguiere, F. (2009). Somatotopic organization of pain responses to direct electrical stimulation of the human insular cortex. *Pain*, *146*, 99–104.
- Mesulam, M. M., & Mufson, E. J. (1982). Insula of the old world monkey. III: Efferent cortical output and comments on function. *The Journal of Comparative Neurology*, *212*, 38–52.
- Moont, R., Crispel, Y., Lev, R., Pud, D., & Yarnitsky, D. (2011). Temporal changes in cortical activation during conditioned pain modulation (CPM), a LORETA study. *Pain*, *152*, 1469–1477.
- Mufson, E. J., & Mesulam, M. M. (1982). Insula of the old world monkey. II: Afferent cortical input and comments on the claustrum. *The Journal of Comparative Neurology*, *212*, 23–37.
- Mufson, E. J., Mesulam, M. M., & Pandya, D. N. (1981). Insular interconnections with the amygdala in the rhesus monkey. *Neuroscience*, *6*, 1231–1248.
- Mugler, J. P., 3rd, & Brookeman, J. R. (1991). Rapid three-dimensional T1-weighted MR imaging with the MP-RAGE sequence. *Journal of Magnetic Resonance Imaging*, *1*, 561–567.
- Navratilova, E., & Porreca, F. (2014). Reward and motivation in pain and pain relief. *Nature Neuroscience*, *17*, 1304–1312.
- Oertel, B. G., & Lotsch, J. (2013). Clinical pharmacology of analgesics assessed with human experimental pain models: Bridging basic and clinical research. *British Journal of Pharmacology*, *168*, 534–553.
- Oertel, B. G., Preibisch, C., Martin, T., Walter, C., Gamer, M., Deichmann, R., & Lötsch, J. (2012). Separating brain processing of pain from that of stimulus intensity. *Human Brain Mapping*, *33*, 883–894.
- Ogawa, S., Lee, T. M., Kay, A. R., & Tank, D. W. (1990). Brain magnetic resonance imaging with contrast dependent on blood oxygenation. *Proceedings of the National Academy of Sciences of the United States of America*, *87*, 9868–9872.
- R Development Core Team. (2008). R: A language and environment for statistical computing.
- Ring, C., Kavussanu, M., & Willoughby, A. R. (2013). Emotional modulation of pain-related evoked potentials. *Biological Psychology*, *93*, 373–376.
- Rolls, E. T., & Grabenhorst, F. (2008). The orbitofrontal cortex and beyond: From affect to decision-making. *Progress in Neurobiology*, *86*, 216–244.
- Rousseeuw, P. J. (1987). Silhouettes: A graphical aid to the interpretation and validation of cluster analysis. *Computational and Applied Mathematics*, *20*, 53–65.
- Spearman, C. (1904). The proof and measurement of association between two things. *The American Journal of Psychology*, *15*, 72–101.
- Starr, C. J., Sawaki, L., Wittenberg, G. F., Burdette, J. H., Oshiro, Y., Quevedo, A. S., & Coghill, R. C. (2009). Roles of the insular cortex in the modulation of pain: Insights from brain lesions. *The Journal of Neuroscience*, *29*, 2684–2694.
- Steen, K. H., Reeh, P. W., Anton, F., & Handwerker, H. O. (1992). Protons selectively induce lasting excitation and sensitization to mechanical stimulation of nociceptors in rat skin, in vitro. *The Journal of Neuroscience*, *12*, 86–95.
- Talbot, J. D., Marrett, S., Evans, A. C., Meyer, E., Bushnell, M. C., & Duncan, G. H. (1991). Multiple representations of pain in human cerebral cortex. *Science*, *251*, 1355–1358.
- Thürauf, N., Ditterich, W., & Kopal, G. (1994). Different sensitivity of pain-related chemosensory potentials evoked by stimulation with CO₂, tooth pulp event-related potentials, and acoustic event-related potentials to the tranquilizer diazepam. *British Journal of Clinical Pharmacology*, *38*, 545–555.
- Tölle, T. R., Kaufmann, T., Siessmeier, T., Lautenbacher, S., Berthele, A., Munz, F., ... Bartenstein, P. (1999). Region-specific encoding of sensory and affective components of pain in the human brain: A positron emission tomography correlation analysis. *Annals of Neurology*, *45*, 40–47.
- Tracey, I., Ploghaus, A., Gati, J. S., Clare, S., Smith, S., Menon, R. S., & Matthews, P. M. (2002). Imaging attentional modulation of pain in the periaqueductal gray in humans. *The Journal of Neuroscience*, *22*, 2748–2752.

- Tzourio-Mazoyer, N., Landeau, B., Papathanassiou, D., Crivello, F., Etard, O., Delcroix, N., ... Joliot, M. (2002). Automated anatomical labeling of activations in SPM using a macroscopic anatomical parcellation of the MNI MRI single-subject brain. *NeuroImage*, *15*, 273–289.
- Walter, C., Oertel, B. G., Felden, L., Kell, C. A., Noth, U., Vermehren, J., ... Lotsch, J. (2016). Brain mapping-based model of delta(9)-tetrahydrocannabinol effects on connectivity in the pain matrix. *Neuropsychopharmacology*, *41*, 1659–1669.
- Ward, J. H., Jr. (1963). Hierarchical grouping to optimize an objective function. *Journal of the American Statistical Association*, *58*, 236–244.
- Warnes, G. R., Bolker, B., Bonebakker, L., Gentleman, R., Liaw, W. H. A., Lumley, T., ... Venables, B. (2020). *gplots: Various R Programming Tools for Plotting Data*. R package version 3.0.4. <https://CRAN.R-project.org/package=gplots>
- Wickham, H. (2016). *ggplot2: Elegant graphics for data analysis*. New York: Springer-Verlag. Retrieved from <https://ggplot2.tidyverse.org>
- Wiech, K., Lin, C. S., Brodersen, K. H., Bingel, U., Ploner, M., & Tracey, I. (2010). Anterior insula integrates information about salience into perceptual decisions about pain. *The Journal of Neuroscience*, *30*, 16324–16331.
- Winston, J. S., Vlaev, I., Seymour, B., Chater, N., & Dolan, R. J. (2014). Relative valuation of pain in human orbitofrontal cortex. *The Journal of Neuroscience*, *34*, 14526–14535.
- Worsley, K. J., & Friston, K. J. (1995). Analysis of fMRI time-series revisited—again. *NeuroImage*, *2*, 173–181.

How to cite this article: Lötsch J, Oertel BG, Felden L, et al. Central encoding of the strength of intranasal chemosensory trigeminal stimuli in a human experimental pain setting. *Hum Brain Mapp*. 2020;41:5240–5254. <https://doi.org/10.1002/hbm.25190>